

# Chromoanasythetic Genomic Rearrangement Identified in a *N-Ethyl-N-Nitrosourea* (ENU) Mutagenesis Screen in *Caenorhabditis elegans*

Omar A. Itani,<sup>\*,†,‡,1</sup> Stephane Flibotte,<sup>§</sup> Kathleen J. Dumas,<sup>\*,†,‡,2</sup> Donald G. Moerman,<sup>§</sup> and Patrick J. Hu<sup>\*,†,‡,3</sup>

<sup>\*</sup>Institute of Gerontology, <sup>†</sup>Department of Internal Medicine, and <sup>‡</sup>Department of Cell and Developmental Biology, University of Michigan Medical School, Ann Arbor, Michigan 48109, and <sup>§</sup>Department of Zoology, University of British Columbia, Vancouver, British Columbia V6T 1Z3, Canada

**ABSTRACT** Chromoanasythesis is a recently discovered phenomenon in humans with congenital diseases that is characterized by complex genomic rearrangements (CGRs) resulting from aberrant repair of catastrophic chromosomal damage. How these CGRs are induced is not known. Here, we describe the structure and function of *dpDp667*, a causative CGR that emerged from a *Caenorhabditis elegans* dauer suppressor screen in which animals were treated with the point mutagen *N-ethyl-N-nitrosourea* (ENU). *dpDp667* comprises nearly 3 Mb of sequence on the right arm of the X chromosome, contains three duplications and one triplication, and is devoid of deletions. Sequences from three out of the four breakpoint junctions in *dpDp667* reveal microhomologies that are hallmarks of chromoanasythetic CGRs. Our findings suggest that environmental insults and physiological processes that cause point mutations may give rise to chromoanasythetic rearrangements associated with congenital disease. The relatively subtle phenotype of animals harboring *dpDp667* suggests that the prevalence of CGRs in the genomes of mutant and/or phenotypically unremarkable animals may be grossly underestimated.

## KEYWORDS

chromo-  
anasythesis  
chromothripsis  
*C. elegans*  
insulin-like  
growth factor  
signaling  
dauer

The incorporation of whole genome sequencing (WGS) into human disease bioanalytic pipelines has led to unexpected insights into the roles of complex genomic rearrangements (CGRs) in the pathogenesis of cancer and congenital disease. The genomes of a significant minority of cancers, and of some patients with congenital abnormalities, harbor

CGRs that are thought to result from a catastrophic “chromosome shattering” event known as chromothripsis (Kloosterman *et al.* 2011, 2012; Stephens *et al.* 2011; Zack *et al.* 2013). These rearrangements are surprisingly complex and can result in tumor suppressor inactivation, oncogene amplification, and other abnormalities that may provide cells with a selective advantage during oncogenesis (Molenaar *et al.* 2012; Northcott *et al.* 2012; Rausch *et al.* 2012; Morin *et al.* 2013; Zack *et al.* 2013; Nones *et al.* 2014; George *et al.* 2015). Chromothriptic CGRs can consist of hundreds of rearrangements, are usually localized to one or a few chromosomes, and exhibit copy number changes that alternate between high and low copy number states, with frequent loss of heterozygosity (LOH). Breakpoint junctions in chromothriptic CGRs typically lack homology, suggesting that they are products of nonhomologous end joining (NHEJ). (Kloosterman *et al.* 2011, 2012; Stephens *et al.* 2011; Holland and Cleveland 2012; Kloosterman and Cuppen 2013; Zhang *et al.* 2013; Weckselblatt and Rudd 2015). A similar but distinct class of CGRs identified in patients with congenital developmental disorders is characterized by localized duplications and triplications without LOH. Sequence analysis of these breakpoint junctions reveals short stretches of homology that are signatures of templated DNA repair rather than NHEJ. These CGRs are thought to be

Copyright © 2016 Itani *et al.*

doi: 10.1534/g3.115.024257

Manuscript received October 28, 2015; accepted for publication November 28, 2015; published Early Online November 30, 2015.

This is an open-access article distributed under the terms of the Creative Commons Attribution 4.0 International License (<http://creativecommons.org/licenses/by/4.0/>), which permits unrestricted use, distribution, and reproduction in any medium, provided the original work is properly cited.

Supporting information is available online at [www.g3journal.org/lookup/suppl/doi:10.1534/g3.115.024257/-/DC1](http://www.g3journal.org/lookup/suppl/doi:10.1534/g3.115.024257/-/DC1)

<sup>1</sup>Present address: Department of Anesthesiology and Pain Medicine, University of Washington School of Medicine, Box 356540, 1959 NE Pacific Street, BB-1469, Seattle, WA 98105

<sup>2</sup>Present address: Buck Institute for Research on Aging, 8001 Redwood Boulevard, Novato, CA 94945

<sup>3</sup>Corresponding author: 3027 Biomedical Science Research Building, 109 Zina Pitcher Place, Ann Arbor, MI 48109-2200. E-mail: [pathu@umich.edu](mailto:pathu@umich.edu)

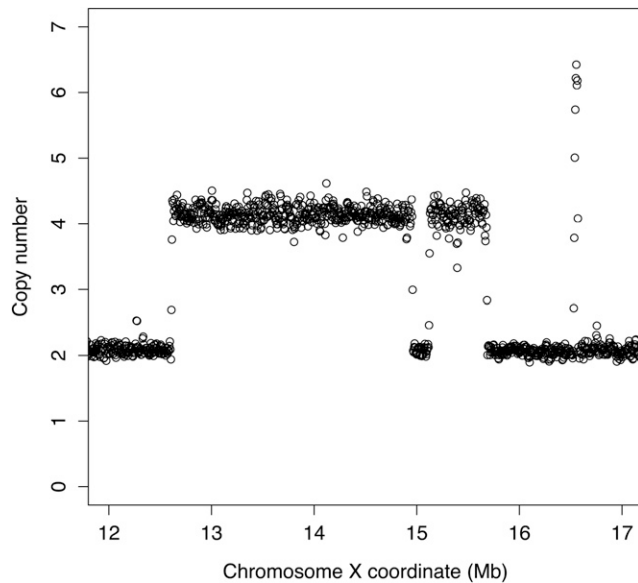


**Figure 1** Copy number estimates based on analysis of whole genome sequencing reads from the right arm of the X chromosome. Each circle represents a genomic window of 10 kb. See *Materials and Methods* for details.

the product of a phenomenon distinct from chromothripsis known as chromoanasythesis (Liu *et al.* 2011; Holland and Cleveland 2012; Kloosterman *et al.* 2012; Kloosterman and Cuppen 2013; Zhang *et al.* 2013; Weckselblatt and Rudd 2015). While catastrophic DNA damage is thought to be a prerequisite for the generation of both classes of CGRs, the inciting events that induce such damage *in vivo* are poorly understood.

Here, we report the analysis of a causative CGR with characteristics of chromoanasythesis that emerged from a *N*-ethyl-*N*-nitrosourea (ENU)-based genetic screen for suppressors of dauer arrest in the nematode *Caenorhabditis elegans*.

## MATERIALS AND METHODS

### C. elegans strains and maintenance

Animals were maintained at 15° on nematode growth media (NGM) plates seeded with *Escherichia coli* OP50. Compound mutants were constructed using standard genetic techniques. Genotypes were confirmed by PCR amplification to detect restriction fragment length or PCR polymorphisms. Percival I-36NL incubators (Percival Scientific, Inc., Perry, IA) were used for maintenance and dauer arrest assays. The following mutant alleles were used in this study: *eak-7(tm3188)* (Alam *et al.* 2010), *akt-1(ok525)* (Hertweck *et al.* 2004), and *daf-2(e1368)* (Kimura *et al.* 1997).

### Suppressor of *eak-7*;*akt-1* (*seak*) screen

The forward genetic screen, WGS, and mapping were performed as previously described (Dumas *et al.* 2013). Animals were exposed to 0.5 mM ENU for 4 hr at room temperature.

### Sequence analysis

Paired-end sequence reads were mapped to the *C. elegans* reference genome version WS230 ([www.wormbase.org](http://www.wormbase.org)) using both short-read aligners BWA (Li and Durbin 2009) and Phaster (Philip Green, personal communication). The resulting alignment files were sorted and

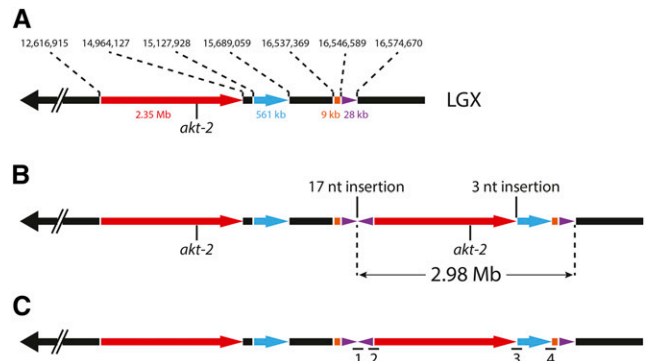


**Figure 2** X chromosome schematics. (A) Schematic of the wild-type X chromosome (LGX). Nucleotide coordinates that define boundaries of rearranged genomic segments (colored) and approximate sizes of these segments are denoted above and below the schematic, respectively. 9 and 28 kb segments are not drawn to scale. The location of the *akt-2* gene is shown. (B) Proposed structure of the *dpDp667* CGR (complex genomic rearrangement). Although the inverted segments flanking the 17-nucleotide insertion are depicted as identical, the two segments actually end at slightly different points in the X chromosome sequence. See Figure 4 for details. (C) Location of four breakpoints unique to *dpDp667*. Primers used to amplify breakpoint junction sequences are shown in Table S1, and genomic sequences spanning each breakpoint are shown in Figure 4.

indexed, and single nucleotide variants (SNVs) were identified with the help of the SAMtools toolbox (Li *et al.* 2009). Copy numbers were estimated in a given genomic interval by dividing the number of aligned reads for strain BQ13 by the number of reads in the corresponding interval for the parental strain, after proper rescaling to a common total number of aligned reads for each library. The estimated copy number in overlapping intervals was examined visually using R ([www.r-project.org](http://www.r-project.org)), and the size of the intervals was varied in order to find the approximate location of each breakpoint. The creation of those overlapping intervals and the calculation of the number of reads within each interval were performed with the BEDTools suite (Quinlan and Hall 2010). Using the IGV genome viewer (Robinson *et al.* 2011; Thorvaldsdottir *et al.* 2013), read alignments around the approximate breakpoints were examined for multiple split-reads with alignments ending at the same location, with the second part of those reads all starting to align at a common location and orientation. In order to confirm the exact breakpoints and junctions found in IGV, a subset of split reads overlapping the junctions were realigned on the reference genome using Blast (Altschul *et al.* 1990) as implemented on WormBase ([www.wormbase.org](http://www.wormbase.org)).

### Polymerase chain reaction (PCR)

PCR was performed using Phusion DNA polymerase (New England BioLabs Inc., Ipswich, MA) according to the manufacturer's protocol. Products were visualized after electrophoresis on a 2% agarose gel containing 0.5 µg/ml ethidium bromide in 1 × Tris-acetate-EDTA (TAE) buffer (primer sequences are provided in Supporting Information, Table S1).

### Dauer arrest assays

Dauer assays were performed at 25° as previously described (Hu *et al.* 2006). Briefly, animals were synchronized in a 4 hr egg-lay at 15° and grown at 25° on NGM plates. Animals were scored

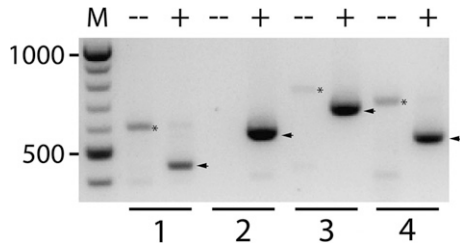


**Figure 3** PCR amplification of junction sequences spanning breakpoints 1–4. Predicted sizes of PCR (polymerase chain reaction) fragments are shown in Table S1. For each set of breakpoint junction primers, template DNA isolated from wild-type (–) and *dpDp667* (+) animals was used. Products from *dpDp667* animals (arrows) were extracted from the gel and subjected to Sanger sequencing to verify sequences flanking each breakpoint. (\*), nonspecific products amplified from wild-type template; M, molecular weight markers.

~60–72 hr after egg-lay. In assays that did not involve RNAi (Figure 5A), animals were fed *E. coli* OP50, and RNAi-based assays (Figure 5B) were conducted using the *E. coli* HT115 feeding RNAi strain (Kamath *et al.* 2001).

## RESULTS AND DISCUSSION

In *C. elegans*, a conserved insulin receptor (InsR)/PI 3-kinase/Akt pathway controls larval development and adult life span (Murphy and Hu 2013). Under replete conditions, agonist insulin-like peptides (ILPs) promote reproductive development by activating the InsR ortholog DAF-2, resulting in activation of the serine-threonine kinases AKT-1 and AKT-2, Akt-dependent phosphorylation of the FoxO transcription factor DAF-16, and subsequent inhibition of DAF-16/FoxO through its export from the nucleus and sequestration in the cytoplasm. In unfavorable environments, antagonist ILPs reduce DAF-2/InsR signaling, thus inducing the translocation of unphosphorylated DAF-16/FoxO to the nucleus, where it promotes larval arrest in a state of diapause known as dauer (Murphy and Hu 2013). *daf-2/InsR* loss-of-function mutants undergo dauer arrest constitutively in a *daf-16/FoxO*-dependent manner (Vowels and Thomas 1992; Gottlieb and Ruvkun 1994).

We discovered a conserved protein of unknown function known as EAK-7 that acts in parallel to AKT-1 to inhibit DAF-16/FoxO-dependent dauer arrest and life span extension (Alam *et al.* 2010). In order to identify new DAF-16/FoxO regulators, we performed an ENU mutagenesis screen for suppressors of the dauer-constitutive phenotype

of *eak-7;akt-1* double mutants (*seak* mutants). This screen previously revealed a new role for the dosage compensation protein DPY-21 in the regulation of dauer arrest and DAF-16/FoxO activity (Dumas *et al.* 2013).

We subjected all *seak* mutants and the parental *eak-7;akt-1* double mutant strain to WGS. The *seak* phenotype in one mutant strain that emerged from this screen, BQ13, mapped just to the right of an ENU-induced noncoding SNV at ~11.9 Mb on the reference X chromosome sequence ([www.wormbase.org](http://www.wormbase.org)). Among 24 recombinants between this SNV and an ENU-induced SNV in the *rgs-11* gene at ~14.9 Mb on the right arm of the X chromosome, no recombination was detected between ENU-induced SNVs in the *R09A8.2* and *elt-3* genes, located at ~12.6 Mb and ~13.9 Mb (corresponding to genetic positions of 7.26 and 15.54 map units), respectively. This observation indicated that the *R09A8.2* and *elt-3* SNVs were in linkage disequilibrium and suggested that BQ13 contained a genomic rearrangement in this region that suppresses recombination between *R09A8.2* and *elt-3*.

Analysis of sequencing read depth from the right arm of the X chromosome in the BQ13 sample revealed two regions of copy number doubling spanning approximately 2 Mb and 500 kb, and one smaller region of apparent copy number tripling (Figure 1). Inspection of individual reads revealed four distinct breakpoint junctions in BQ13, each of which was identified in multiple reads. None of these hybrid reads was present in the parental *eak-7;akt-1* samples. These data were consistent with the presence of a CGR on the right arm of the X chromosome (Figure 2). To verify the proposed structure of this CGR, PCR primers were designed to amplify each of the four predicted breakpoint junctions in BQ13 (Figure 2C and Table S1). Each primer set amplified a fragment of the predicted size (Table S1) from BQ13 genomic DNA but not from wild-type genomic DNA (Figure 3), and Sanger sequencing of these PCR products verified breakpoint sequences identified in WGS reads (Figure 4). In accordance with conventions of *C. elegans* nomenclature [(Horvitz *et al.* 1979); Tim Schedl, personal communication], we refer to this CGR as *dpDp667*, since the rearrangement consists mostly of duplicated sequence.

*dpDp667* has two main features that suggest it is a product of chromoanasythesis rather than chromothripsis. First, it contains three duplications and a triplication but does not harbor any deletions. This contrasts with the typical alternation of high and low copy number states that is seen in chromothripsis (Stephens *et al.* 2011; Holland and Cleveland 2012; Kloosterman and Cuppen 2013; Zhang *et al.* 2013; Weckselblatt and Rudd 2015). Furthermore, breakpoint junctions 1 and 3 contain short insertions that are homologous to

- 1 X:16574485(+) -> X:16574670(-)  
 TGGGAATGCAAACTTGAAGTTTCTCTG**ACTTGAAGTTTCTCTG**AGAAAAAACTATGAAAATTTGTTTTCCATGTTAAAGTTAAAG
- 2 X:12616918(-) -> X:16546586(+)  
 TTATATTCCTATTATAGAAAGATTGTCITGGATTGGAATTTTCATAGTGCCTAAAGCATTATCCGACGTTCTTTCCATCCAAAAGTTTGGTC
- 3 X:14964127(+) -> X:15127928(+)  
 GGCTTTTCATAGTCAACTTGTGAATGAAGTCCCGTTTGA**GAA**GAC**GAA**GACTTTGAAATGAGAGCATTCTTGATCTTTGACACATTTTTCT
- 4 X:15689059(+) -> X:16537369(+)  
 ATGTCGTGGCTCAACAAAATAATGCCGAGGAGACATTGGCGAGGATAATTGA**ACTTCTGAGTTGTTGTTTCTGGTTCTATTGATAATGTT**

**Figure 4** Breakpoint junction sequences. X chromosome coordinates of the nucleotides adjacent to the breakpoint are shown above each sequence. (+): positive DNA strand; (–): negative DNA strand. Junctional insertions in breakpoints 1 and 3 are in black, emboldened, and underlined, and junctional sequences homologous to these insertions are emboldened and underlined. An AGT triplet present at the ends of both fusion partners of breakpoint junction 2 is in purple, emboldened, and underlined. See text for details.

nearby junctional sequences, and junction 2 contains a triplet that is present at both ends of the breakpoint (Figure 4). These findings suggest that these three fusions are products of templated DNA repair, which is a characteristic of chromoanasyntetic CGRs (Liu *et al.* 2011; Holland and Cleveland 2012; Kloosterman and Cuppen 2013; Zhang *et al.* 2013; Weckselblatt and Rudd 2015). It is conceivable that the cellular machinery responsible for generating chromoanasyntetic CGRs in the germline is conserved between humans and *C. elegans*.

Due to their complexity, the functional significance of most reported CGRs has not been ascertained experimentally. In a previous study, we showed that mutations in *dpy-21*, the first gene to emerge from our *seak* screen, suppress the dauer-constitutive phenotypes of *eak-7;akt-1* double mutants and *daf-2/InsR* mutants at least in part by increasing *akt-2* expression (Dumas *et al.* 2013). Since the *akt-2* gene is duplicated in *dpDp667* (Figure 2), we hypothesized that *dpDp667* suppresses dauer arrest by increasing *akt-2* gene dosage.

As AKT-2 acts in the DAF-2/InsR pathway to prevent dauer arrest and promote reproductive development (Paradis and Ruvkun 1998), we first tested the ability of *dpDp667* to suppress the dauer-constitutive phenotype of the *daf-2(e1368)* mutant (Kimura *et al.* 1997). *dpDp667* suppressed the dauer-constitutive phenotypes of both *daf-2(e1368)* mutants as well as *eak-7;akt-1* double mutants (Figure 5A). We then directly tested the role of *akt-2* in dauer suppression by *dpDp667*. If *dpDp667* suppresses dauer arrest by increasing *akt-2* gene dosage, then RNAi knockdown of *akt-2* should increase the penetrance of dauer arrest in *daf-2;dpDp667* animals. *akt-2* RNAi did not induce dauer arrest at 25° in wild-type animals but did cause partially penetrant dauer arrest in *akt-1* mutant animals (Figure 5B), indicating that *akt-2* RNAi reduced *akt-2* activity (Paradis and Ruvkun 1998). In contrast to complete suppression of the *daf-2(e1368)* dauer-constitutive phenotype by *dpDp667* observed when grown on the standard *E. coli* OP50 strain, *daf-2;dpDp667* animals had a partially penetrant dauer-constitutive phenotype when grown on the HT115 feeding RNAi strain (compare Figure 5, A and B). This is likely a consequence of the influence of *E. coli* strain-specific differences on dauer arrest (Ferguson *et al.* 2013). *akt-2* RNAi strongly enhanced the penetrance of dauer arrest in *daf-2;dpDp667* animals (Figure 5B). Therefore, we conclude that *dpDp667* suppresses the dauer-constitutive phenotype of *daf-2/InsR* mutants at least in part through increased *akt-2* gene dosage. We cannot exclude the possibility that increased dosage of other genes in *dpDp667* also contributes to the dauer suppression phenotype.

Although progress has been made in understanding the biogenesis of CGRs (Crasta *et al.* 2012; Zhang *et al.* 2015), the initial events leading to chromothripsis and chromoanasyntesis are poorly understood. Recent work in *C. elegans* suggests that CGRs can be induced in wild-type animals by the alkylating agent mechlorethamine (Meier *et al.* 2014). Our discovery of a causative CGR in a ENU-based genetic screen was unexpected, given the propensity of ENU to cause point mutations (Flibotte *et al.* 2010). This finding suggests that, in principle, CGRs could arise from any physiological or pathological process that causes point mutations. Since ENU can induce large copy-number duplications/deletions at low frequency *in vivo* [~0.3%; (Thompson *et al.* 2013)], an alternative model is that *dpDp667* arose from a rare double-strand break induced by ENU. We also cannot exclude the possibility that this CGR arose spontaneously, albeit in the context of a genetic screen.

The discovery of chromothripsis and chromoanasyntesis was a direct consequence of the use of WGS to analyze the genomes of cancer cells (Stephens *et al.* 2011) and patients with congenital

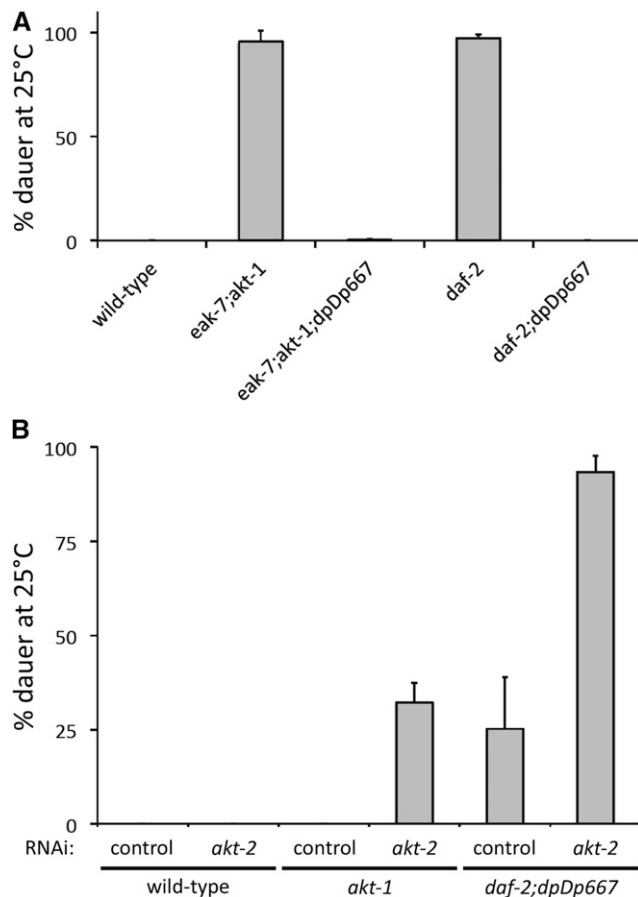


**Figure 5** *dpDp667* suppresses dauer arrest in an *akt-2*-dependent manner. (A) *dpDp667* suppresses the dauer-constitutive phenotype of *eak-7;akt-1* double mutants and *daf-2* single mutants. (B) Suppression of the dauer-constitutive phenotype of *daf-2* mutants by *dpDp667* requires *akt-2*. See text for details. Both panels show composite results from three independent trials. Error bars represent standard deviation. RNAi, RNA interference.

developmental abnormalities (Kloosterman *et al.* 2011; Liu *et al.* 2011). Here, we report the first detailed structure of a chromoanasyntetic rearrangement in *C. elegans* that causes a mutant phenotype. The structures of CGRs in *C. elegans* had not been reported prior to the advent of WGS. This is likely due to difficulties in resolving the structures of CGRs in the absence of WGS data, as well as the known bias of commonly used mutagens such as ENU and ethyl methanesulfonate (EMS) toward point mutations (Flibotte *et al.* 2010). In line with the mutagenic spectrum of EMS and ENU, WGS analytic pipelines are typically optimized for the identification of SNVs (Doitsidou *et al.* 2010; Zuryn *et al.* 2010).

As the BQ13 mutant strain that emerged from our screen does not appear to have gross phenotypic abnormalities, it is likely that other mutants that have been isolated from forward genetic screens but have not been subjected to WGS may harbor cryptic causative CGRs that are well tolerated by the organism. Such CGRs have already been documented in humans (Bertelsen *et al.* 2015; de Pagter *et al.* 2015). Furthermore, it is possible that the structure of previously described simple rearrangements, most of which have not been analyzed using WGS, may be more complex than previously appreciated. In all of these situations, analysis of read depth (Figure 1) would likely reveal evidence of a cryptic CGR. Therefore, we advocate the routine

incorporation of read depth analysis into WGS pipelines. As WGS has now become a standard tool in the analysis of mutant genomes (Hu 2014), we anticipate the discovery of many more CGRs as the underlying cause of mutant phenotypes in *C. elegans* and other organisms.

## ACKNOWLEDGMENTS

Some strains were provided by the *Caenorhabditis* Genetics Center, which is funded by the National Institutes of Health (NIH) Office of Research Infrastructure Programs (P40 OD010440). This work was supported by a Postdoctoral Fellowship from the American Heart Association (O.A.I.), the Biology of Aging Training Grant (T32AG000114) awarded to the University of Michigan Geriatrics Center by the National Institute on Aging (K.J.D.), the Canadian Institute for Health Research (D.G.M.), Research Scholar Grant DDC-119640 from the American Cancer Society (P.J.H.), and R01 grant AG041177 from the NIH (P.J.H.). D.G.M. is a senior fellow of the Canadian Institute for Advanced Research.

## LITERATURE CITED

- Alam, H., T. W. Williams, K. J. Dumas, C. Guo, S. Yoshina *et al.*, 2010 EAK-7 controls development and life span by regulating nuclear DAF-16/FoxO activity. *Cell Metab.* 12: 30–41.
- Altschul, S. F., W. Gish, W. Miller, E. W. Myers, and D. J. Lipman, 1990 Basic local alignment search tool. *J. Mol. Biol.* 215: 403–410.
- Bertelsen, B., L. Nazaryan-Petersen, W. Sun, M. M. Mehrjouy, G. Xie *et al.*, 2015 A germline chromothripsis event stably segregating in 11 individuals through three generations. *Genet. Med.* (in press).
- Crasta, K., N. J. Ganem, R. Dagher, A. B. Lantermann, E. V. Ivanova *et al.*, 2012 DNA breaks and chromosome pulverization from errors in mitosis. *Nature* 482: 53–58.
- de Pagter, M. S., M. J. van Roosmalen, A. F. Baas, I. Renkens, K. J. Duran *et al.*, 2015 Chromothripsis in healthy individuals affects multiple protein-coding genes and can result in severe congenital abnormalities in offspring. *Am. J. Hum. Genet.* 96: 651–656.
- Doitsidou, M., R. J. Poole, S. Sarin, H. Bigelow, and O. Hobert, 2010 *C. elegans* mutant identification with a one-step whole-genome-sequencing and SNP mapping strategy. *PLoS One* 5: e15435.
- Dumas, K. J., C. E. Delaney, S. Flibotte, D. G. Moerman, G. Csankovszki *et al.*, 2013 Unexpected Role for Dosage Compensation in the Control of Dauer Arrest, Insulin-Like Signaling, and FoxO Transcription Factor Activity in *Caenorhabditis elegans*. *Genetics* 194: 619–629.
- Ferguson, A. A., S. Roy, K. N. Kormanik, Y. Kim, K. J. Dumas *et al.*, 2013 TATN-1 mutations reveal a novel role for tyrosine as a metabolic signal that influences developmental decisions and longevity in *Caenorhabditis elegans*. *PLoS Genet.* 9: e1004020.
- Flibotte, S., M. L. Edgley, I. Chaudhry, J. Taylor, S. E. Neil *et al.*, 2010 Whole-genome profiling of mutagenesis in *Caenorhabditis elegans*. *Genetics* 185: 431–441.
- George, J., J. S. Lim, S. J. Jang, Y. Cun, L. Ozretic *et al.*, 2015 Comprehensive genomic profiles of small cell lung cancer. *Nature* 524: 47–53.
- Gottlieb, S., and G. Ruvkun, 1994 *daf-2*, *daf-16* and *daf-23*: genetically interacting genes controlling Dauer formation in *Caenorhabditis elegans*. *Genetics* 137: 107–120.
- Hertweck, M., C. Gobel, and R. Baumeister, 2004 *C. elegans* SGK-1 is the critical component in the Akt/PKB kinase complex to control stress response and life span. *Dev. Cell* 6: 577–588.
- Holland, A. J., and D. W. Cleveland, 2012 Chromoanagenesis and cancer: mechanisms and consequences of localized, complex chromosomal rearrangements. *Nat. Med.* 18: 1630–1638.
- Horvitz, H. R., S. Brenner, J. Hodgkin, and R. K. Herman, 1979 A uniform genetic nomenclature for the nematode *Caenorhabditis elegans*. *Mol. Gen. Genet.* 175: 129–133.
- Hu, P. J., 2014 Whole genome sequencing and the transformation of *C. elegans* forward genetics. *Methods* 68: 437–440.
- Hu, P. J., J. Xu, and G. Ruvkun, 2006 Two membrane-associated tyrosine phosphatase homologs potentiate *C. elegans* AKT-1/PKB signaling. *PLoS Genet.* 2: e99.
- Kamath, R. S., M. Martinez-Campos, P. Zipperlen, A. G. Fraser and J. Ahringer, 2001 Effectiveness of specific RNA-mediated interference through ingested double-stranded RNA in *Caenorhabditis elegans*. *Genome Biology* 2: RESEARCH0002.
- Kimura, K. D., H. A. Tissenbaum, Y. Liu, and G. Ruvkun, 1997 *daf-2*, an insulin receptor-like gene that regulates longevity and diapause in *Caenorhabditis elegans*. *Science* 277: 942–946.
- Kloosterman, W. P., and E. Cuppen, 2013 Chromothripsis in congenital disorders and cancer: similarities and differences. *Curr. Opin. Cell Biol.* 25: 341–348.
- Kloosterman, W. P., V. Guryev, M. van Roosmalen, K. J. Duran, E. de Bruijn *et al.*, 2011 Chromothripsis as a mechanism driving complex de novo structural rearrangements in the germline. *Hum. Mol. Genet.* 20: 1916–1924.
- Kloosterman, W. P., M. Tavakoli-Yaraki, M. J. van Roosmalen, E. van Binsbergen, I. Renkens *et al.*, 2012 Constitutional chromothripsis rearrangements involve clustered double-stranded DNA breaks and non-homologous repair mechanisms. *Cell Reports* 1: 648–655.
- Li, H., and R. Durbin, 2009 Fast and accurate short read alignment with Burrows-Wheeler transform. *Bioinformatics* 25: 1754–1760.
- Li, H., B. Handsaker, A. Wysoker, T. Fennell, J. Ruan *et al.*, 2009 The Sequence Alignment/Map format and SAMtools. *Bioinformatics* 25: 2078–2079.
- Liu, P., A. Erez, S. C. Nagamani, S. U. Dhar, K. E. Kolodziejska *et al.*, 2011 Chromosome catastrophes involve replication mechanisms generating complex genomic rearrangements. *Cell* 146: 889–903.
- Meier, B., S. L. Cooke, J. Weiss, A. P. Bailly, L. B. Alexandrov *et al.*, 2014 *C. elegans* whole-genome sequencing reveals mutational signatures related to carcinogens and DNA repair deficiency. *Genome Res.* 24: 1624–1636.
- Molenaar, J. J., J. Koster, D. A. Zwijnenburg, P. van Sluis, L. J. Valentijn *et al.*, 2012 Sequencing of neuroblastoma identifies chromothripsis and defects in neurogenesis genes. *Nature* 483: 589–593.
- Morin, R. D., K. Mungall, E. Pleasance, A. J. Mungall, R. Goya *et al.*, 2013 Mutational and structural analysis of diffuse large B-cell lymphoma using whole-genome sequencing. *Blood* 122: 1256–1265.
- Murphy, C. T., and P. J. Hu, 2013 Insulin/insulin-like growth factor signaling in *C. elegans* (December 26, 2013). *WormBook* ed. The *C. elegans* Research Community WormBook, doi/10.1895/wormbook.1.164.1, <http://www.wormbook.org>.
- Nones, K., N. Waddell, N. Wayte, A. M. Patch, P. Bailey *et al.*, 2014 Genomic catastrophes frequently arise in esophageal adenocarcinoma and drive tumorigenesis. *Nat. Commun.* 5: 5224.
- Northcott, P. A., D. J. Shih, J. Peacock, L. Garzia, A. S. Morrissy *et al.*, 2012 Subgroup-specific structural variation across 1,000 medulloblastoma genomes. *Nature* 488: 49–56.
- Paradis, S., and G. Ruvkun, 1998 *Caenorhabditis elegans* Akt/PKB transduces insulin receptor-like signals from AGE-1 PI3 kinase to the DAF-16 transcription factor. *Genes Dev.* 12: 2488–2498.
- Quinlan, A. R., and I. M. Hall, 2010 BEDTools: a flexible suite of utilities for comparing genomic features. *Bioinformatics* 26: 841–842.
- Rausch, T., D. T. Jones, M. Zapatka, A. M. Stutz, T. Zichner *et al.*, 2012 Genome sequencing of pediatric medulloblastoma links catastrophic DNA rearrangements with TP53 mutations. *Cell* 148: 59–71.
- Robinson, J. T., H. Thorvaldsdottir, W. Winckler, M. Guttman, E. S. Lander *et al.*, 2011 Integrative genomics viewer. *Nat. Biotechnol.* 29: 24–26.
- Stephens, P. J., C. D. Greenman, B. Fu, F. Yang, G. R. Bignell *et al.*, 2011 Massive genomic rearrangement acquired in a single catastrophic event during cancer development. *Cell* 144: 27–40.
- Thompson, O., M. Edgley, P. Strasbourger, S. Flibotte, B. Ewing *et al.*, 2013 The million mutation project: a new approach to genetics in *Caenorhabditis elegans*. *Genome Res.* 23: 1749–1762.

- Thorvaldsdottir, H., J. T. Robinson, and J. P. Mesirov, 2013 Integrative Genomics Viewer (IGV): high-performance genomics data visualization and exploration. *Brief. Bioinform.* 14: 178–192.
- Vowels, J. J., and J. H. Thomas, 1992 Genetic analysis of chemosensory control of dauer formation in *Caenorhabditis elegans*. *Genetics* 130: 105–123.
- Weckselblatt, B., and M. K. Rudd, 2015 Human Structural Variation: Mechanisms of Chromosome Rearrangements. *Trends Genet.* 31: 587–599.
- Zack, T. I., S. E. Schumacher, S. L. Carter, A. D. Cherniack, G. Saksena *et al.*, 2013 Pan-cancer patterns of somatic copy number alteration. *Nat. Genet.* 45: 1134–1140.
- Zhang, C. Z., M. L. Leibowitz, and D. Pellman, 2013 Chromothripsis and beyond: rapid genome evolution from complex chromosomal rearrangements. *Genes Dev.* 27: 2513–2530.
- Zhang, C. Z., A. Spektor, H. Cornils, J. M. Francis, E. K. Jackson *et al.*, 2015 Chromothripsis from DNA damage in micronuclei. *Nature* 522: 179–184.
- Zuryn, S., S. Le Gras, K. Jamet, and S. Jarriault, 2010 A strategy for direct mapping and identification of mutations by whole-genome sequencing. *Genetics* 186: 427–430.

*Communicating Editor: D. S. Fay*